



## Experimental investigation of pore clogging by microparticles: Evidence for a critical flux density of particle yielding arches and deposits

Gbedo Constant Agbangla <sup>a,b,e</sup>, Éric Climent <sup>c,d,e</sup>, Patrice Bacchin <sup>a,b,e,\*</sup>

<sup>a</sup> Université de Toulouse, INPT, UPS Laboratoire de Génie Chimique, 118 Route de Narbonne, F-31062 Toulouse, France

<sup>b</sup> CNRS, UMR 5503, F-31062 Toulouse, France

<sup>c</sup> Université de Toulouse, INPT, UPS, Institut de Mécanique des Fluides, Allée Camille Soula, F-31400 Toulouse, France

<sup>d</sup> CNRS, UMR 5502, F-31400 Toulouse, France

<sup>e</sup> CNRS, Fédération de recherche FERMAT, Toulouse, France

### ARTICLE INFO

#### Article history:

Received 14 February 2012

Received in revised form 25 August 2012

Accepted 7 September 2012

Available online 21 September 2012

#### Keywords:

Channel  
Clogging  
Plugging  
Microparticle  
Colloidal interactions  
Deposition

### ABSTRACT

Prediction of pore fouling by microparticles is still challenging and remains a difficult step to optimize membrane and filtration processes. The scientific issue consists in determining the relevant operation parameters controlling the capture of particles and the clogging of the filter. In this study, we have developed for a dead-end and cross-flow filtration a poly-dimethylsiloxane (PDMS) device which allows direct observation of the clogging dynamics of microchannels (20 µm wide) by micrometric particles (5 µm diameter). The experiments highlight the formation of different 3D clogging patterns according to the filtration conditions (particle concentration, flowrate, particle flux density and physical-chemical conditions of suspension). Besides, we have determined under which specific conditions of filtration, the latex microparticles are captured and form arches, clusters or dendrites. For each type of structure, the temporal dynamics of the particle deposition are analyzed by means of the average thickness of deposit. The critical conditions for the formation of arches leading to deposit formation have been identified in term of a combination of operating conditions: the particle concentration and the particle velocity. A critical particle flux density yielding pore clogging is then observed and characterized. Studying these experimental results helps to identify pore clogging mechanisms: deposition, interception and bridging.

© 2012 Elsevier B.V. All rights reserved.

### 1. Introduction

For separation processes such as microfiltration or ultrafiltration, one of the most stringent issues is the clogging of the porous material which reduces the process efficiency [1] and increases energy consumption. To reduce or prevent the impact of filter or membrane fouling, it is necessary to understand how these phenomena occur and how they are influenced by operating conditions of the process (i.e. the filtered dispersion, the filter, and the filtering conditions).

In former experimental and numerical studies, it has been shown that filter clogging or membrane fouling is controlled by a complex interplay between the drag force acting on particles (due to permeation velocity [2]), direct hydrodynamic interactions (e.g. shear induced diffusion), the properties of particles [3] and particle/particle or particle/wall non-hydrodynamic surface interactions [4]. For micrometric particles, it has been shown that the

colloidal interaction plays an important role in fouling and clogging events. A major consequence of this is the existence of a critical filtration velocity which yields fouling or clogging (when drag force overcomes the double layer electrostatic repulsion barrier). This has been identified by Ramachandran and Fogler [5] while they investigated the conditions of multilayer deposition in microchannels and by Field et al. [6] and Bacchin et al. [2] when they found membrane filtration conditions preventing deposit formation. In spite of several numerical and experimental investigations, there are still important discrepancies between experimental observations and model predictions of critical velocities [7]. The main causes for these discrepancies are related to a complex and collective particle behavior (due to multi-body particle interactions) at the pore scale that cannot be described yet by classical Lagrangian or Eulerian modeling [4].

In order to progress towards a better understanding and description of clogging mechanisms, it is then necessary to have a direct access to experimental information at the pore scale [8] (whereas in past decades the investigations were based on the global variation of operating conditions like the filtrate flux and pressure drop on the whole filter or membrane surface). Recently, the direct visualization of micropore fouling has been made

\* Corresponding author at: Université de Toulouse, INPT, UPS Laboratoire de Génie Chimique, 118 Route de Narbonne, F-31062 Toulouse, France.

E-mail addresses: [gbedoconstant@yahoo.fr](mailto:gbedoconstant@yahoo.fr) (G.C. Agbangla), [eric.climent@imft.fr](mailto:eric.climent@imft.fr) (É. Climent), [bacchin@chimie.ups-tlse.fr](mailto:bacchin@chimie.ups-tlse.fr) (P. Bacchin).

possible by new progresses in the micro-device fabrication technology [9]. Mustin and Stoeber [10] have investigated the effect of particle sizes (between  $0.47\text{ }\mu\text{m}$  and  $1.5\text{ }\mu\text{m}$ ) on the dynamics of microsystem clogging by means of filtration experiments carried out at a constant pressure drop. According to the size distribution of particles in suspension, they concluded that deposit of particles leading to the microsystem clogging occurs through successive particle deposits, particle size exclusion, or through a combination of these effects. Sharp and Adrian [11], by means of experiments in microtubes, have observed blockage due to arches formation. The experiments were carried out with liquids seeded with polystyrene latex beads at very low volumetric concentration. They showed that a stable balance between the hydrodynamic forces and the contact forces (friction) between particles and the wall can lead to the formation of stable arches. Wyss et al. [8] have studied the clogging of PDMS microchannels by aqueous suspensions of monodisperse polystyrene beads. The formation of clogs in the microchannel occurred when a critical number of particles was flowing through the pore whatever the flowrate and the particle volume fraction.

In this context, our contribution to the study of pore fouling is to investigate the dynamic capture and deposition of particles at a pore entrance by using an experimental approach (experimental devices similar to those presented in [4,8]) for dead-end and cross-flow filtration of latex suspensions. Then, this manuscript reports on different particle concentration, flowrate of suspensions (filtration velocity), particle flux density and physical-chemical conditions (effect of additional salt).

The paper is organized as follows. A brief description of the experimental technique, visualization procedure and quantification of the average thickness of particle deposit is given in Section 2. In Section 3, we investigate the kinetics of clogging characterized by the evolution of average thickness of deposit on plug imaging. The effects of particle concentration, filtration flowrate and physical-chemical properties of latex particle suspensions on clogging are also discussed. In Section 4, we identify the experimental parameters leading to the capture and deposit of particles and analyze the dynamics of this deposition.

## 2. Description of experiments

### 2.1. Materials

From an experimental point of view, a key to breakthrough in understanding fouling phenomena is the development of novel, non-invasive, *in situ* quantification of physical-chemical interactions occurring during filtration [12]. To answer to this need, we developed poly-dimethylsiloxane (PDMS) microfluidic devices to mimic filtration systems. It consists in the elaboration of micro-separators (microsystems) in PDMS designed by usual soft lithography technique [13]. The transparent device associated with digital video microscopy allows a direct observation of latex particles and deposit formation within the microseparator during filtration. Our device consists in parallel arrangement of several 27 microchannels being  $20\text{ }\mu\text{m}$  wide (to mimic a set of ideal pores in a filter). The distance between the centers of two successive microchannels is  $70\text{ }\mu\text{m}$  and the total filtration length is equal to  $1.94\text{ mm}$ . The depth of all microchannels is  $50\text{ }\mu\text{m}$  and their length is  $200\text{ }\mu\text{m}$ . Then, the value of filtration surface  $S$  in front of microchannels is equal to  $0.097\text{ mm}^2$  for all filtration experiments. A partial view of our microsystem is shown in Fig. 1 where the direction of the flowing suspension can be parallel to the filtration area (to mimic cross-flow filtration) or perpendicular to the area (to mimic dead-end filtration). The PDMS microsystems are periodically rinsed with ultra-pure deionized water.

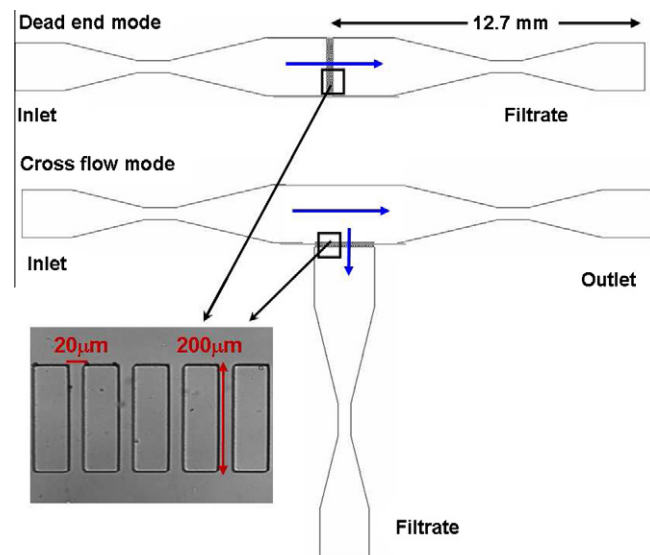


**Fig. 1.** Schematic view of the PDMS micro-separators used for dead-end and cross-flow filtration.

For this study, we used monosized polystyrene microspheres (Sulfate latex 4% v/v Invitrogen Molecular Probes) dispersed in pure water. These spherical negatively charged particles have a diameter equal to  $4.9\text{ }\mu\text{m} \pm 0.21$ . Particles are smaller than the width of microchannel pores. For filtration experiments, they are dispersed either in ultra-pure water or in a KCl solution. When particles are dispersed in salt solution (KCl concentration typically equal to  $10^{-1}\text{ M}$  in our investigation), the magnitude of the electrostatic interaction between particles and the PDMS wall is reduced. This KCl concentration is lower than the critical salt concentration in a quiescent fluid ( $2.10^{-1}\text{ M}$ ) in order to avoid the aggregation of particles. Prior to filtration, the latex suspensions are sonicated and then observed under the microscope to verify the absence of particle aggregation.

### 2.2. Filtration technique and visualization procedure

These PDMS devices allow a direct observation (thanks to a video or a confocal microscopy with a magnification of  $100\times$ ) of the clogging of microchannels by microparticles. For each set of experiments, the particle suspension is injected in the device with a fixed volumetric concentration (ratio between the volume of latex particles and the volume of filtrated suspension). Different values of the flowrate are imposed through the microchannel by the syringe pump (Sky Electronic PS 2000). The microsystem is placed on the platform of an Axiolab (Zeiss) microscope (see Fig. 2). The visualization

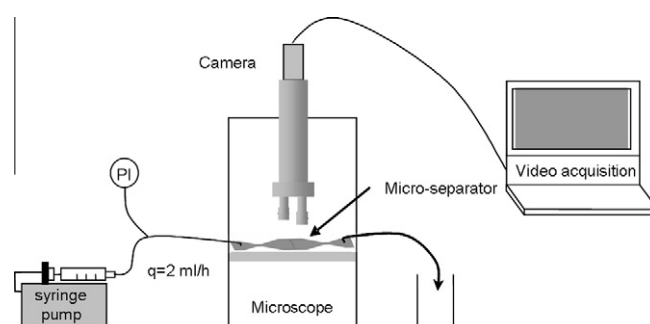


**Fig. 2.** Experimental set-up for imaging the channel blockage.

alization of particles capture and deposit in dead-end or cross-flow filtration has been recorded by using highly sensitive camera (Pixelfly QE, PCQ). This camera is connected to the computer for image storage, data processing and results analysis. The dynamics of the particle capture and deposit are recorded by grabbing images every 20 s of filtration. The temporal evolution of the average thickness of the particle deposit is analyzed for all experiments.

### 2.3. Average thickness of particle deposit

The application of the thresholding technique which has been made possible thanks to the ImageJ software helps to quantify the surface occupied by the deposited particles present in the microsystem. The binarization of the obtained images, facilitated by the strong contrast between the adhered particles and the rest of the microsystem image, allows to determine the number of pixels occupied by the PDMS wall and deposited particles. The number of pixels corresponding to the first recorded image (image with microchannels only) has been subtracted from the pixel values of other images recorded in time in order to take into account the deposited particles. This normalized number of pixels is then converted to surface ( $\text{mm}^2$  in particular) due to the known dimensions for engravings present in the microsystem: 1 mm corresponds to 783 pixels. The ratio between the surface of deposited particles and the length of the filtration zone (1.94 mm) equals the average thickness of deposit.

## 3. Operating conditions and experimental results

A set of experiments has been carried out in order to analyze the clogging of microchannels by different patterns of deposit structures formed by microparticles (5  $\mu\text{m}$  diameter). These experiments are performed under various conditions:

- the volume fraction ( $\phi$ ) of particles is varied: between  $5.10^{-4}$  and  $5.10^{-3}$ ,
- the flowrate  $q$  of suspension is varied between  $0.4 \text{ ml h}^{-1}$  and  $20 \text{ ml h}^{-1}$  corresponding to an average flow velocity in the feeding channel ranging from  $1.2 \text{ mm s}^{-1}$  to  $57 \text{ mm s}^{-1}$ . Under those flow conditions, the Reynolds number ranges between 0.024 and 1.14 corresponding to laminar flows.

The Stokes number of particles associated to these experimental conditions is very small ranging between  $8.10^{-5}$  and  $4.10^{-3}$ . Thus, inertial effects of particle dynamics are negligible. The diffusion of latex particles is also negligible because the Peclet number is very high ranging between  $0(10^4$  and  $10^6)$ . Finally, the sedimentation of particles can be neglected because the sedimentation time of particles (50 s) in the depth of microchannels is much longer than the residence time ( $10^{-2} \text{ s}$  for  $q = 2 \text{ ml h}^{-1}$ ) of particles in the microchannel.

The results obtained by varying the volume fraction of particles, the filtration flowrate and the physical-chemical conditions of the suspension are analyzed in the following subsections.

### 3.1. Effect of particle concentration

At a constant flowrate ( $q = 2 \text{ ml h}^{-1}$ ), the volume fraction of latex suspensions has an important effect on the capture mechanism. After 90 min of filtration, no particle capture is observed when the volume fraction of particles dispersed in pure water is  $10^{-3}$  (Fig. 3) whereas particle capture is clearly occurring when latex suspension concentration is increased to  $5.10^{-3}$  (see Fig. 4 where dark regions are related to a local increase of the particle deposit). The formation of these cluster structures does not occur

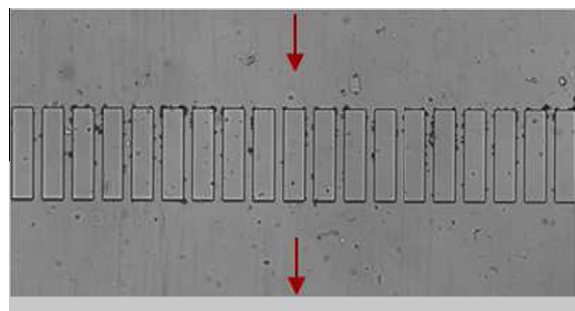


**Fig. 3.**  $\phi = 10^{-3} \text{ v/v}$ ;  $q = 2 \text{ ml h}^{-1}$ : no deposit of particles after 90 min of dead-end filtration. Latex suspensions are dispersed in ultra-pure water.

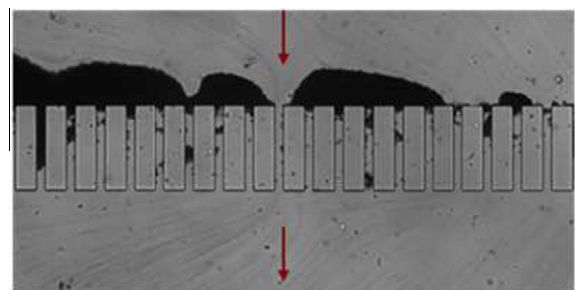


**Fig. 4.**  $\phi = 5.10^{-3} \text{ v/v}$ ;  $q = 2 \text{ ml h}^{-1}$ : cluster formation after 90 min of dead-end filtration. Latex suspensions are dispersed in ultra-pure water.

homogeneously in the channel but depends strongly on the interplay between the local fluid velocity (forcing particle wall interaction) and the 3D development of the structure (which perturbs the flow). When the volume fraction of particles increased, the flux of latex particles passing through the microchannel entrance was increased. For both experiments, it can be noted that a slight variation in particle concentration induces a dramatic change in microchannel clogging. There is a critical particle volume fraction ( $\phi$  between  $10^{-3}$  and  $5.10^{-3}$ ) under which no deposit of particle is observed. Iscan and Civan [14] have already discussed about the effect of particle concentrations on fouling mechanism. They conclude that a high volume fraction of particles may plug pore and perforations (by bridging across during various well operations including particle-containing water injections and workover activities) in unfavorable flow conditions. Ramachandran and Fogler [5] also analyzed this feature (the pore clogging) as an increase of the probability of bridging (several particles blocking simultaneously the entrance) when the concentration of particles increases. This mechanism could explain the sudden appearance of the clogging for particle concentration above  $\phi = 5.10^{-3}$ .

In order to study the dynamic of the clogging, image analysis are performed in order to obtain the temporal variation of the average thickness of deposited particles. Fig. 5 presents the evolution of the average thickness of deposit for two volume fractions of particle during the dead-end filtration. For volume fraction  $\phi = 10^{-3}$ , the temporal evolution of the average thickness remains low (0.018 mm at  $t = 90 \text{ mm}$ ). It means that no significant fouling is occurring in the microsystem. For  $\phi = 5.10^{-3}$ , the value of this average thickness increases quickly to 0.18 mm during 90 min (the duration of the experiment). This is a clear evidence of particle deposits formation during the filtration. An average thickness of deposit equal to 180  $\mu\text{m}$  corresponds to a multilayer (around 36 layers) of particles with 5  $\mu\text{m}$  in diameter. These particle structures correspond to the cluster observed in Fig. 4. A slope breaking is observed for a high volume fraction of particles ( $\phi = 5.10^{-3}$ ). As it

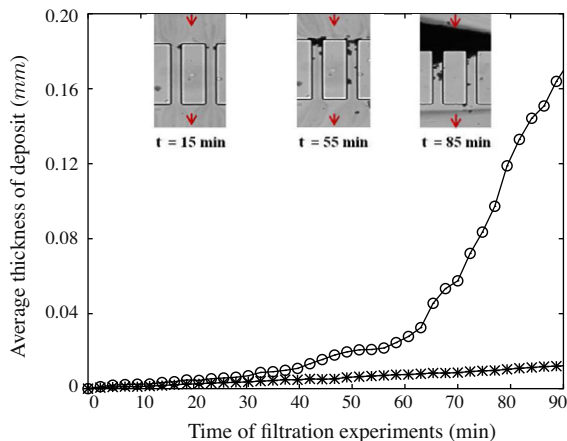


**Fig. 5.** The temporal evolution of the average thickness of particle deposit:  $\phi = 10^{-3}$  v/v;  $q = 2 \text{ ml h}^{-1}$ , and  $\phi = 5.10^{-3}$  v/v;  $q = 2 \text{ ml h}^{-1}$  (dispersed in ultra-pure water) with snapshots of the cluster formation at  $t = 15, 55$  and  $85$  min.

will be further discussed in Section 4, this sudden increase can be attributed to the change from arches formation to a rapid deposition (cluster formation) of different particle structures.

### 3.2. Effect of the filtration flowrate

To study the effect of the suspension flowrate in the deposition process of microparticles and yielding clogging of microchannels, the volume fraction ( $\phi$ ) of latex particles is kept fixed (equal to  $10^{-3}$ ). During filtration experiments, the flowrate has been changed (from  $2 \text{ ml h}^{-1}$  to  $10 \text{ ml h}^{-1}$ ). The results in terms of average thickness of deposit show again an important formation of particle deposit for experiment carried out at  $q = 10 \text{ ml h}^{-1}$  (Fig. 6) while no deposit of particle is observed for the flowrate  $q = 2 \text{ ml h}^{-1}$ . Indeed, increasing the flowrate enhances hydrodynamic forcing which allows particles to overcome more easily the repulsion barrier and brings them to strong adhesion. The important deposit of particle obtained at  $q = 10 \text{ ml h}^{-1}$  results in a rapid increase of the average thickness of deposit reaching  $0.58 \text{ mm}$  over  $40 \text{ min}$  of filtration as shown in Fig. 7.

Increasing the flowrate or the volume fraction of particles (previous subsection) lead to an important formation of particle clusters over time. In the discussion section, the existence of a critical particle flux density (product of the flow velocity and the particle volume fraction) for particle deposition will be presented.

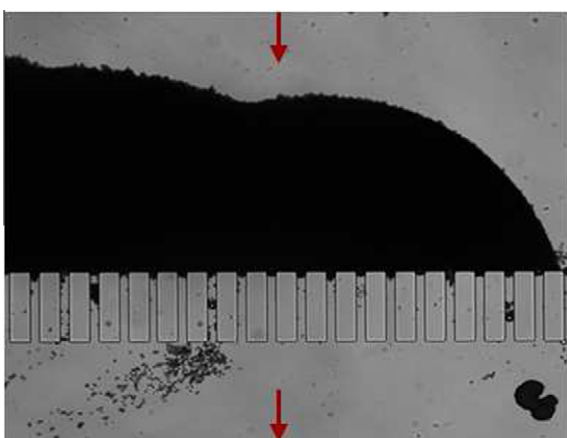


**Fig. 6.**  $\phi = 10^{-3}$  v/v;  $q = 10 \text{ ml h}^{-1}$ : cluster formation after  $40$  min of dead-end filtration. Latex suspensions are dispersed in ultra-pure water.

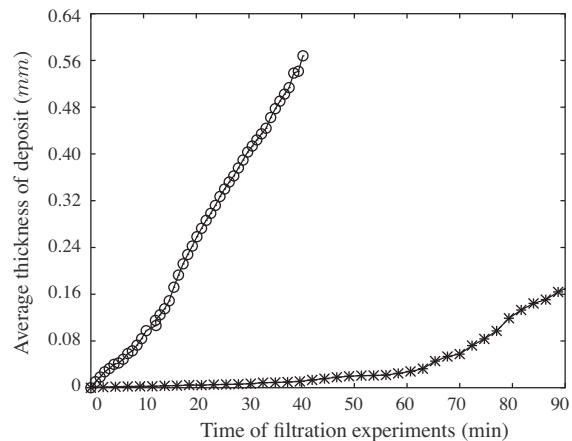


**Fig. 7.** The temporal evolution of the average thickness of particle deposit:  $\phi = 5.10^{-3}$  v/v;  $q = 2 \text{ ml h}^{-1}$ , and  $\phi = 10^{-3}$  v/v;  $q = 10 \text{ ml h}^{-1}$  (dispersed in ultra-pure water).

### 3.3. Physical-chemical effect on deposit structure

The influence of the physical-chemical properties of the latex suspensions on the particle deposition is analyzed in this section. To determine the role of this physical-chemical effects in the deposition process, latex particles are dispersed in KCl solution at  $10^{-1} \text{ M}$  for different particulate volume fractions. This reduces repulsion barriers although the suspension remains stable in a quiescent fluid. At a constant flowrate  $q = 2 \text{ ml h}^{-1}$ , we have already mentioned that under a volume fraction  $\phi = 5.10^{-3}$  no deposit of particle has been observed when latex suspensions are dispersed in ultra-pure water. However, particle structures are clearly identified above  $\phi = 5.10^{-4}$  (see Fig. 8) when suspensions are dispersed in KCl solution. The electrostatic repulsive interaction between the particles is reduced within water-KCl solutions; this facilitates the deposition of particles. For particles dispersed in KCl solution at  $10^{-1} \text{ M}$ , different fouling patterns can be observed when the different parameters are varied. For latex dispersions, it leads to the formation of dendrites attached onto the channel walls. The formation of these dendrites is influenced by the flow direction (streamlines orientation): straight and tilted dendrites are obtained respectively in dead-end filtration (see Fig. 9) and cross-flow filtration (see Fig. 10). The dendrites length for  $\phi = 10^{-3}$  can reach more than  $100 \mu\text{m}$ , i.e.  $20$  particle diameters after  $90 \text{ min}$ . The formations of dendritic structures have already been observed by Payatakes and Gradon [15], but the mechanism has not been clearly understood yet.

Fig. 11 indicates that the average thickness of deposit remains almost unchanged for  $\phi = 10^{-3}$ ;  $q = 2 \text{ ml h}^{-1}$  in the case of sus-

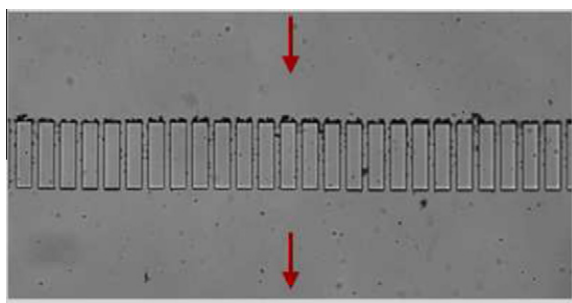


**Fig. 8.**  $\phi = 5.10^{-4}$  v/v;  $q = 2 \text{ ml h}^{-1}$ : early instants of dendrites formation after  $90$  min of dead-end filtration. Latex suspensions are dispersed in KCl-water solution at  $10^{-1} \text{ M}$ .

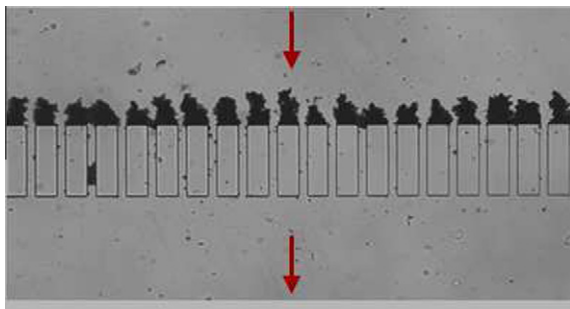


**Fig. 9.**  $\phi = 10^{-3}$  v/v;  $q = 2 \text{ ml h}^{-1}$ : formation of straight dendrites after 90 min of dead-end filtration. Latex particles are dispersed in KCl-water solution at  $10^{-1}$  M.

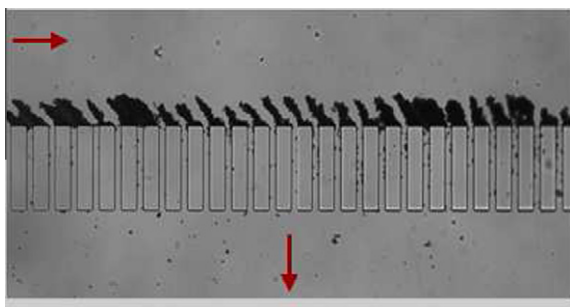


**Fig. 10.**  $\phi = 10^{-3}$  v/v;  $q = 2 \text{ ml h}^{-1}$ : formation of tilted dendrites after 90 min of cross-flow filtration. Latex particles are dispersed in KCl-water solution at  $10^{-1}$  M.

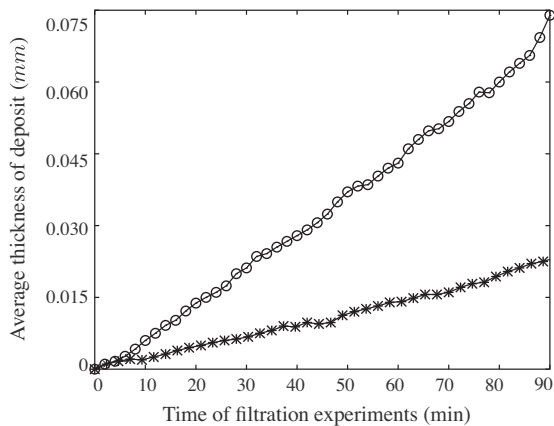


**Fig. 11.** The temporal evolution of the average thickness of particle deposit:  $--\phi = 10^{-3}$  v/v;  $q = 2 \text{ ml h}^{-1}$  (dispersed in ultra-pure water), and  $--\phi = 10^{-3}$  v/v;  $q = 2 \text{ ml h}^{-1}$  (dispersed in KCl at  $10^{-1}$  M).

pensions dispersed in ultra-pure water. However, this average thickness increases to 0.075 mm (due to dendrites formation) in 90 min for the experiment performed at  $\phi = 10^{-3}$ ;  $q = 2 \text{ ml h}^{-1}$  when particles are dispersed in salt solution. These experiments illustrate that colloidal interactions can play a significant role in the capture of micrometric particles.

#### 4. Discussion

The experimental results obtained under dead-end or cross-flow filtration conditions with an imposed flowrate show the dependence of the clogging on various conditions such as the volumetric concentration of latex particles, flowrate of suspensions and physical-chemical conditions (summarized in Fig. 12). Changing physical-chemical conditions (adding salt in the suspension)

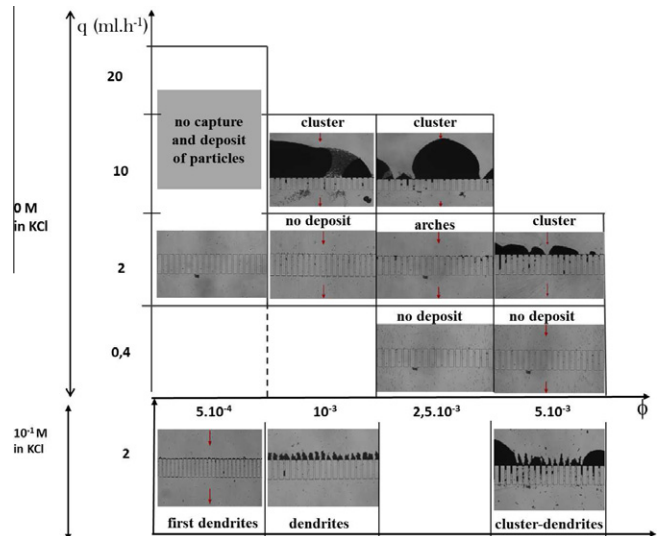


**Fig. 12.** Summary of different deposit structures of latex particles formed during filtration experiments. For  $q \leq 2 \text{ ml h}^{-1}$ , images are taken after 90 min of filtration while experiments performed at  $q = 10 \text{ ml h}^{-1}$  last only 40 min.

plays a role on the particle deposit and on the shape of deposit structures (dendrite formation) at low volume fraction. This effect of surface interactions tends to disappear when the volume fraction of particles is significantly increased. It has been possible to form clusters and dendrites simultaneously under the same configuration by increasing the concentration of particles for suspension dispersed in salt solution. The transition towards cluster formation seems to appear for the same operating condition when particles are suspended in ultra-pure water or salt solution.

In fact, increasing the volume fraction (up to  $\phi = 5.10^{-3}$ ) and the flowrate (up to  $q = 10 \text{ ml h}^{-1}$ ) leads the microsystem to experience a transition: clean microsystem without deposit towards channel blockage by clusters. These features are possibly related to the collective effect of particles (high volume fraction of particles:  $\phi = 5.10^{-3}$ ) and to the important hydrodynamic forcing (high flowrate:  $q = 10 \text{ ml h}^{-1}$ ) during the clogging mechanism. Indeed, increasing the volume fraction of suspensions induces a significant enhancement of bridging events for deposition whereas increasing the flowrate induces an important hydrodynamic forcing which helps latex particles to overcome their repulsive barrier yielding adhesion.

#### 4.1. Critical conditions of particle deposit

Different filtration experiments have been carried out by varying the volume fraction of particles dispersed in ultra-pure water and the flow velocity in suspension. Each experimental condition where the combined effect of both volume fraction and flow velocity has been studied. For dead-end filtration, all results can be gathered in a single Fig. 13. Filled diamond symbols refer to particle deposition and clogging while open circles correspond to the absence of clogging during our experiments. No clogging of microsystem is observed for a volume fraction of particles lower than  $5.10^{-4}$  whatever the values of average flow velocity. Likewise, a minimum value of the flow velocity is needed to induce the capture and deposition of particles at high volume fraction. Varying the particle concentration or the average flow velocity influences the behavior of particles. Based on this observation, we then consider the response of the system to the product  $V_{\text{moy}} \cdot \phi$  which represents the particle flux density through the microchannel entrance area. The average thickness of particle deposit is thus represented in

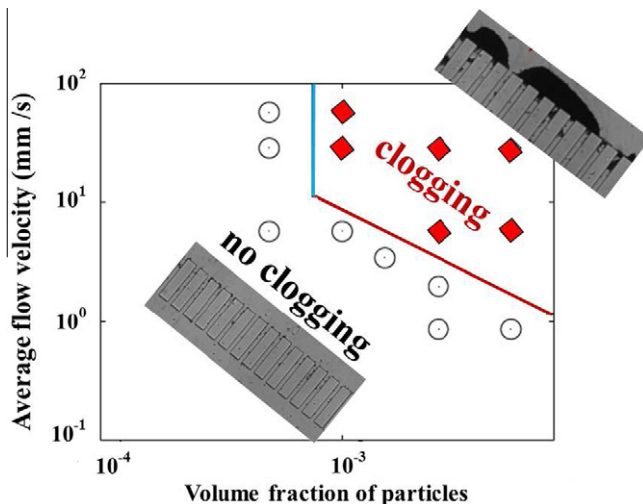


**Fig. 13.** Experimental conditions leading to deposition of latex particles and to the microsystem clogging. Results shown in this figure represent the state of microsystem after 90 min of filtration performed by dispersing the latex particles in ultra-pure water and varying the volume fraction of particles and the average flow velocity: filled diamonds: clogging, open circles: no clogging.

**Fig. 14** according to the product  $V_{\text{moy}} \cdot \phi$  for each experimental condition mentioned below:

- in \* :  $\phi = 5.10^{-4}$  and  $V_{\text{moy}} = (5.7, 28.5, 57) \text{ mm s}^{-1}$ ,
- in  $\diamond$  :  $\phi = 10^{-3}$  and  $V_{\text{moy}} = (5.7, 28.5, 57) \text{ mm s}^{-1}$ ,
- in  $\circ$  :  $\phi = 2.510^{-3}$  and  $V_{\text{moy}} = (1.2, 5.7, 28.5) \text{ mm s}^{-1}$ , and
- in + :  $\phi = 5.10^{-3}$  and  $V_{\text{moy}} = (1.2, 5.7) \text{ mm s}^{-1}$ .

When the average thickness of the particle deposit reaches ten particle diameters, we consider that clogging occurs. This value corresponds experimentally to the formation of arches at the pore scale (Fig. 5). The presence of arches leads to definite and complete clogging of the microsystem. Results shown in Fig. 14 confirm the existence of a critical flux density leading to the particle deposition and to the microsystem clogging. This critical value is estimated between  $4.10^{-3} \text{ mm s}^{-1}$  and  $5.10^{-3} \text{ mm s}^{-1}$  during the dead-end filtration of repulsive latex particles ( $5 \mu\text{m}$  in diameter) dispersed in ultra-pure water.

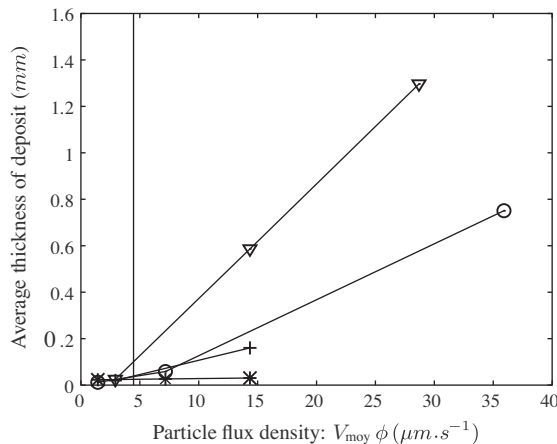


**Fig. 14.** Determination of a critical flux density of particle leading to the deposition and to the microsystem clogging after 90 min of dead-end filtration. Each symbol corresponds to a different volume fraction of latex particles dispersed in ultra-pure water,  $-*-\phi = 5.10^{-4}$ ,  $-\nabla-\phi = 10^{-3}$ ,  $-\circ-\phi = 2.510^{-3}$ , and  $-+-\phi = 5.10^{-3}$ .

#### 4.2. Arches formation leading to deposit

The dead-end filtration experiments performed at  $\phi = 5.10^{-3}$ ;  $q = 2 \text{ ml h}^{-1}$  and leading to the formation of cluster structures in particle deposition have been observed more precisely focusing on the pore entrance with an optical magnification of  $500\times$ . Far from this micropore, the filtrated suspension dispersed in ultra-pure water remains stable. During 90 min, images showing the positions of latex particles in flow have been recorded at  $12 \text{ frames min}^{-1}$  using a microscope with an optical magnification of  $500\times$ .

During the process of image acquisition, the sudden blockage of the pore entrance can be observed between two successive images at a very short time compared to the total duration of the experiment. Thus, for a filtration time equal to 35 min, Fig. 16 shows several particles arriving simultaneously at the pore entrance and blocking the crossing section which was open 5 s before (Fig. 15). Ramachandran and Fogler [5] have already highlighted this phenomenon called bridging. For filtration experiments of microspheres ( $0.249 \mu\text{m}$  in diameter) through the micropore ( $1 \mu\text{m}$  in wide), they analyzed this feature as an increase of the probability of bridging events (several particles blocking the entrance simultaneously) at a volume fraction of particles (PSS latex spheres) equal to  $1.235 \times 10^{-3}$ .

The bridging phenomenon is one among other mechanisms of capture and deposition during the process of microchannel clogging. In addition to the bridging mechanism, one can note another process of particle deposition called progressive capture of particles. It means that particles attach one by one either at a preferential position of micropore [16] at the beginning of filtration experiments or onto another adhered particles. This progressive deposition of particles (highlighted during the filtration of particles

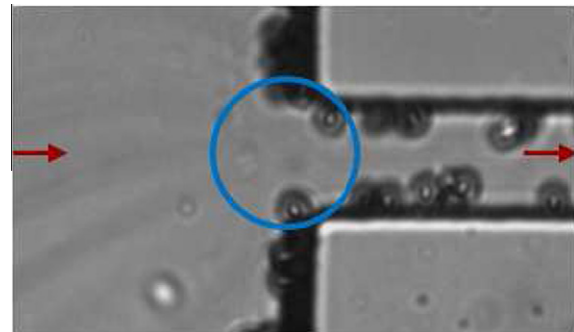


**Fig. 15.** Close-up on the open microchannel entrance after 34 min and 55 s of dead-end filtration ( $\phi = 5 \times 10^{-3}$ ;  $q = 2 \text{ ml h}^{-1}$ ).

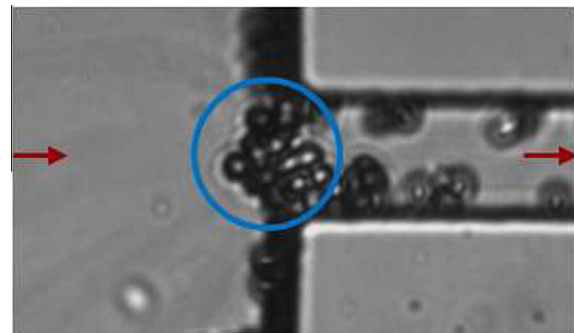


**Fig. 16.** Final state of the bridging mechanism after the passage of 7650 particles through the micropore in 5 s: close-up on particles blocking the microchannel entrance after 35 min of dead-end filtration ( $\phi = 5 \times 10^{-3}$ ;  $q = 2 \text{ ml h}^{-1}$ ).

with low repulsion) leads slowly and to the clogging of microchannels with different aggregate (cluster) structures of particles whereas bridging is a rapid transition.

To confirm definitely the occurrence of bridging in particle deposition, we would need rather to record the microchannel images each 0.5 ms (corresponding to the crossing time of particles through a microchannel with a stable filtrated suspension).

## 5. Conclusion

Our work showed that particle capture and deposit formation during microchannel clogging are depended on the balance between hydrodynamic forces (induced by the flow velocity), the volume fraction of dispersed particles and the physical-chemical surface interactions. A slight change in this balance leads to strikingly different patterns of particle structures and pore clogging aggregates (no deposit, dendrite, arch, dense deposit). Dendritic structures appear when latex suspensions are dispersed in KCl salt solution at  $10^{-1}$  M (i.e. for low particle-particle and particle-wall repulsions). When suspensions are dispersed in ultra-pure water (i.e. strong repulsions), we observe that cluster structures of particles are formed for experiments performed at  $\phi = 5.10^{-3}$ ;  $q = 2 \text{ ml h}^{-1}$  and at  $\phi = 10^{-3}$ ;  $q = 10 \text{ ml h}^{-1}$  whereas no deposit of particles is obtained at  $q = 2 \text{ ml h}^{-1}; \phi = 10^{-3}$ . The evolution of the average thickness of particle deposit also shows a change in the capture and deposit kinetics. For different conditions used in these filtration experiments, we determine and quantify the operating parameters under which no particle capture occurs and above which arches and deposits form. The critical conditions for this transition are a particle volume fraction greater than  $5.10^{-4}$  ( $\phi > 5.10^{-4}$ ) and a particle flux density higher than  $5.10^{-3}$  ( $V_{\text{moy}} \cdot \phi > 5.10^{-3} \text{ mm s}^{-1}$ ). Particle interactions, the effect of hydrodynamics, particle concentration, flowrate and surface interactions are physical parameters controlling the kinetics of membrane clogging during filtration processes. Our experiments show that clogging is the result of collective behaviors of particles at the channel entrance. Numerical simulations accounting for multi-body interactions are needed to model the collective behav-

ior of particles with more details during deposit formation (the clogging transition depends on the concentration).

## References

- [1] G. Belfort, R.H. Davis, A.L. Zydny, The behavior of suspensions and macromolecular solutions in cross-flow microfiltration, *Journal of Membrane Science* 96 (1994) 1–58.
- [2] P. Bacchin, P. Aimar, V. Sanchez, Model for colloidal fouling of membrane, *AIChE Journal* 41 (1995) 368–376.
- [3] A. Iscan, F. Civan, M. Kok, Alteration of permeability by drilling fluid invasion and flow reversal, *Journal of Petroleum Science and Engineering* 58 (2007) 227–244.
- [4] P. Bacchin, A. Marty, P. Duru, M. Meireles, P. Aimar, Colloidal surface interactions and membrane fouling: investigations at pore scale, *Advances in Colloid and Interface Science* 164 (2011) 2–11.
- [5] V. Ramachandran, H.S. Fogler, Plugging by hydrodynamic bridging during flow of stable colloidal particles within cylindrical pores, *Journal of Fluid Mechanics* 385 (1999) 129–156.
- [6] R.W. Field, D. Wu, J.A. Howell, B.B. Gupta, Critical flux concept for microfiltration fouling, *Journal of Membrane Science* 100 (1995) 259–272.
- [7] P. Bacchin, B. Espinasse, Y. Bessiere, D. Fletcher, P. Aimar, Numerical simulation of colloidal dispersion filtration: description of critical flux and comparison with experimental results, *Desalination* 192 (2006) 74–81.
- [8] M.H. Wyss, L.D. Blair, F.J. Morris, A.H. Stone, A.D. Weitz, Mechanism for clogging of microchannels, *Physical Review* 74 (2006) 061402.
- [9] S. Kuiper, C.J.M. van Rijn, W. Nijdam, M.C. Elwenspoek, Developement and applications of very high flux microfiltration membranes, *Journal of Membrane Science* 150 (1998) 1–8.
- [10] B. Mustin, B. Stoeber, Deposition of particles from polydisperse suspensions in microfluidic systems, *Microfluid Nanofluid* 9 (2010) 905–913.
- [11] K.V. Sharp, R.J. Adrian, On flow-blocking particle structures in microtubes, *Microfluid Nanofluid* 1 (2005) 376–380.
- [12] J.C. Chen, Q. Li, M. Elimelech, In situ monitoring techniques for concentration polarization and fouling phenomena in membrane filtration, *Advances in Colloid and Interface Science* 107 (2004) 83–108.
- [13] J.C.M. Donald, D.C. Duffy, J.R. Anderson, D.T. Chiu, H. Wu, G.M. Whitesides, Fabrication of microfluidic systems in poly(dimethylsiloxane), *Electrophoresis* 21 (2000) 27–40.
- [14] A. Iscan, F. Civan, Correlation of criteria perforation and pore plugging by particles, *Journal of Porous Media* 9 (2006) 541–558.
- [15] A. Payatakes, L. Gradon, Dendritic deposition of aerosol by convective brownian diffusion for small, intermediate and high particle knudsen numbers, *AIChE Journal* 26 (1980) 443–454.
- [16] J. Lin, D. Bourrier, M. Dilhan, P. Duru, Particle deposition on a microsieve, *Physics of Fluids* 21 (2009) 073301.